Permutations uniquely identify states and unknown external forces in non-autonomous dynamical systems

Yoshito Hirata, Yuzuru Sato, Davide Faranda

Permutations uniquely identify states and unknown external forces in non-autonomous dynamical systems

Yoshito Hirata,[1,2] Yuzuru Sato,[3,4] and Davide Faranda[5,4]

[1]*Mathematics and Informatics Center/Graduate School of Information Science and Technology/International Research Center for Neurointelligence (WPI-IRCN), The University of Tokyo, 7-3-1 Hongo, Bunkyo-ku, Tokyo 113-8656, Japan*

[2]*Faculty of Engineering, Information and Systems, University of Tsukuba, 1-1-1 Tennodai, Tsukuba, Ibaraki 305-8573, Japan**

[3]*Research Institute for Electronic Science/Department of Mathematics, Hokkaido University, Kita 20 Nishi 10, Kita-ku, Sapporo, Hokkaido 001-0020, Japan*

[4]*London Mathematical Laboratory, 8 Margravine Gardens, Hammersmith, London W6 8RH, UK*

[5]*LSCE-IPSL, CEA Saclay l'Orme des Merisiers, CNRS UMR 8212 CEA-CNRS-UVSQ, Université, Paris-Saclay, 91191, Gif-sur-Yvette, France*

Abstract

It has been shown that a permutation can uniquely identify the joint set of an initial condition and a non-autonomous external force realization added to the deterministic system in given time series data. We demonstrate that our results can be applied to time series forecasting as well as the estimation of common external forces. Thus, permutations provide a convenient description for a time series dataset generated by non-autonomous dynamical systems.

* hirata@cs.tsukuba.ac.jp

The symbolic method is a powerful tool for analyzing time series data by coarse-graining. When the underlying dynamics is deterministic, a generating partition and symbolic dynamics may be used to convert an initial condition to an infinitely long symbolic sequence in a one-to-one manner. However, this method fails for non-autonomous dynamics, e.g. deterministic dynamical systems in the presence of dynamical noise or external forces, because a partition cannot remove the uncertainty in specifying an initial condition. Here, we show that, unlike a generating partition for symbolic dynamics, permutations (ordinal patterns) can represent a real-valued time series generated by non-autonomous dynamical systems. We show that a permutation establishes a one-to-one correspondence with a realized orbit based on the joint set of an initial condition and external force realization added to the deterministic system, if the dynamics under dynamical noise is topologically transitive. Thus, our results explain why permutations, in some cases, can distinguish deterministic systems from stochastic systems. In addition, we demonstrate that our findings can be applied to forecasting behavior as well as estimating common dynamical noise in random dynamical systems.

I. INTRODUCTION

In the analysis of time series data generated by dynamical systems, coarse-graining a state is one of the conventional approaches to describe dynamical systems [1–7]. This procedure is the cornerstone of statistical mechanics and provides a framework to describe several complex physical phenomena such as turbulent flow [8], molecular dynamics [9] among others. For example, in a deterministic dynamical system, a generating partition helps us to establish one-to-one correspondence between an initial condition and the orbit of symbolic dynamics. Subsequently, we can provide rigorous foundations and/or calculations [3, 7] as well as bridge the ideas coming from dynamical systems theory and information theory [10–12]. However, this method fails for stochastic dynamics because any partition cannot remove the uncertainty for a state in the system due to externally added noise [13, 14]. Recently, stochastic chaos in random dynamical systems has been studied theoretically and experi-

mentally [15, 16]. The main finding is the possibility to describe the behavior of complex systems such as turbulent forced flows with simple dynamical systems where non-essential degrees of freedom are lumped in the random dynamics. These studies clearly show the existence of open problems on *nonlinear time series analysis for random / non-autonomous dynamical systems.*

Permutations (or ordinal patterns) or topological methods in nonlinear time series analysis, have been studied as an alternative analysis to coarse-grained dynamics [17]. It is known that we can estimate the Kolmogorov-Sinai entropy not only by generating partitions but also by permutations [18]. Distinguishing deterministic systems from stochastic systems is a recent trend in permutation studies. [19–25]. In physics, the interest is to understand whether a deterministic behavior can be separated from a stochastic dynamics, thus enabling for simpler descriptions of complex systems, as in Ref. [16]. Here, we examine the hypothesis that a permutation can achieve a one-to-one correspondence with a joint set of an initial condition and a realization of the external force in random and non-autonomous dynamical systems, as the length of the permutations tends to infinity. The key idea is that the variety of permutations could grow super-exponentially as the size of permutations increases when the underlying dynamics is stochastic [24, 26]. This super-exponential growth can accommodate the information regarding the state space as well as a stochastic input series within a permutation.

II. OUR SETTINGS AND THEORETICAL RESULTS

We consider a non-autonomous dynamical system $f : X \times P \to X$

$$x_{t+1} = f(x_t, p_t),\ x_t \in X,\ p_t \in P, \tag{1}$$

Here x_t is a model of the state of the dynamical system, and p_t is a model of external force or noise, which drives the dynamical system at time t. Here we adopt both X and P as one-dimensional intervals.

We assume the following [27]:

1. The sequence $\{p_t\}_{t=0,\ldots,n-1}$ is given beforehand as a hidden parameter to be estimated.

2. The function $f(x, p)$ is a continuous map and an embedding in terms of arbitrary p;

Namely, under $x_{t+1} = f(x_t, p)$, the parameter p corresponds to x_{t+1} in a one-to-one manner when we fix x_t.

Our goal is to estimate both x_0 and $\{p_t\}_{t=0,\ldots,n-1}$, based on the given time series data $\{x_t\}_{t=1,\ldots,n}$. Here, as a shorthand, we write $x_{t+1} = f_{p_t}(x_t)$ and

$$x_{t+1} = f_{p_t}(f_{p_{t-1}}(\cdots f_{p_0}(x_0)\cdots) = f_{p_0^t}(x_0), \tag{2}$$

where $p_0^t = \{p_\tau\}_{\tau=0,\ldots,t}$.

We now introduce the permutations [17, 18]. Suppose that a scalar time series s_t ($t = 1, 2, \ldots, N$) is given. Now, consider n consecutive measurements $s_t, s_{t+1}, \ldots, s_{t+n-1}$ starting from time t. If we sort these measurements in the ascending order, we have

$$s_{t+t_1} \leq s_{t+t_2} \leq \cdots \leq s_{t+t_n}, \tag{3}$$

where we define $s_{t+t_i} \leq s_{t+t_j}$, if $s_{t+t_i} = s_{t+t_j}$ and $t_i < t_j$. Then, the obtained series

$$\pi_t(n) = (t_1, t_2, \ldots, t_n) \tag{4}$$

is called the *permutation* for time t with length n. It is known that the Kolmogorov-Sinai entropy can be obtained using permutations if the underlying dynamics is ergodic [18].

We especially consider the dynamics in a one-dimensional space X and introduce a natural measure μ if for all test functions $h : X \to \mathbf{R}$, we have

$$\lim_{N\to\infty} \frac{1}{N} \sum_{t=0}^{N-1} h(f_{p_0^t}(x)) \to \int_A h d\mu \tag{5}$$

for almost all $x \in A \subset X$ and for almost all p_0^t [28]. We further assume that the non-autonomous dynamical system (2) has a natural measure.

We refer to $x_{t+1} = f_{p_0^t}(x_t)$ as topologically transitive if $\{x_t\}$ is dense in $A \subset X$. This definition can be equivalent to that if there exists $t > 0$ such that $f_{p_0^t}(U) \cap V \neq \phi$ for any pair of open sets $U, V \subset A \subset X$. Approximately, when one starts from an open set U, we can visit the neighborhood of another open set V after finite iterations of f. Note that in general, the topological transitivity in random and non-autonomous dynamical systems depends on the given p_0^t. In other words, here we exclude the case where $f_{p_0^t}(x)$ only forms a finite periodic orbit because such an orbit is not dense on A. Our theoretical result is summarized as the following main theorem:

Theorem 1. *Suppose f on X has a natural measure. Let $[x_{i_0^n-1}, x_{i_0^n+1}]$ be an interval for an initial condition x_0 specified by a permutation of length n. Similarly, $[\underline{p}_{t,n}, \bar{p}_{t,n}]$ be an interval for the external force at time t specified by the same permutation. Then, each of $[x_{i_0^n-1}, x_{i_0^n+1}]$ and $[\underline{p}_{t,n}, \bar{p}_{t,n}]$ for each t converges to a single point when the length n of the permutation tends to infinity if and only if the dynamics f on X is topologically transitive.*

The following Lemma 1 and the contraposition of Lemma 2 lead to the above main theorem.

Lemma 1. *Suppose that the dynamics f on X is topologically transitive and has a natural measure. Then, a permutation can specify a joint set of an initial condition x_0 and a realization of the external force $\{p_t\}$ as the length of the permutation goes to infinity. Namely, $[x_{i_0^n-1}, x_{i_0^n+1}]$ and $[\underline{p}_{t,n}, \bar{p}_{t,n}]$ for each t converge to single points, respectively.*

Proof. Suppose that the current length of permutations is n. Additionally, let us assume initially that x_0 is neither the minimum nor the maximum of $x \in X$. Then, if x_0 is the i_0^n-th point from below, the initial value x_0 is sandwiched between the $i_0^n - 1$-th point $x_{i_0^n-1}$ and the $i_0^n + 1$-th point $x_{i_0^n+1}$, namely, we have $x_{i_0^n-1} \leq x_0 \leq x_{i_0^n+1}$, which is an interval between the minimum and the maximum of x. Let us consider $x_{i_0^n-1}$ and $x_{i_0^n+1}$, separately. First, we consider $x_{i_0^n-1}$. Because we assume that the dynamics is topologically transitive, there is $m_L(1) > n$ such that $x_{i_0^{m_L(1)}-1} \in (x_{i_0^n-1}, x_0)$, implying that $x_{i_0^n-1} < x_{i_0^{m_L(1)}-1} < x_0$. By applying the same logic repeatedly, we can choose a sequence $\{m_L(k) : k = 1, 2, \ldots\}$ such that $x_{i_0^{m_L(k)}} < x_{i_0^{m_L(l)}} < x_0$ for $0 < k < l$. Since the sequence of $x_{i_0^{m_L(k)}}$ is always less than x_0 and increasing monotonically, we have $x_{i_0^{m_L(k)}} \to x_0$ when $k \to \infty$. By using the similar logic, there is a sequence $\{m_R(k) : k = 1, 2, \ldots\}$ such that $x_{i_0^{m_R(k)}} > x_{i_0^{m_R(l)}} > x_0$ for $0 < k < l$. Thus, $x_{i_0^{m_R(k)}} \to x_0$ when $k \to \infty$.

Both limits mean that the interval $[x_{i_0^n-1}, x_{i_0^n+1}]$ gets smaller and smaller, and converges to a single point x_0 when the length of permutations tends to infinity. In addition, since the i_0^n-th point among n points can be rephrased as a certain percentile point on μ as a natural measure, the initial condition x_0 can be specified on X. Therefore, the theorem has been proven. When x_0 is either the minimum or the maximum of $x \in X$, we can make x_0 a sandwich within $[\min_{x \in I} x, x_{i_0^n+1}]$ or $[x_{i_0^n-1}, \max_{x \in I} x]$, respectively. Thus, the similar monotonic convergence argument discussed above holds for both cases.

As it has been found that a series of states $\{x_t\}$ is identified by the corresponding permutation, each p_t can be inferred because now we assume that $f(x_t, p)$ is an embedding in terms of the arbitrary non-autonomous force p given x_t. Therefore, if f is known, we can identify the joint set of $\{x_t\}$ and $\{p_t\}$ by the corresponding permutation as the length of permutations tending to infinity. □

Lemma 2. *Suppose that the dynamics f on a one-dimensional space X is not topologically transitive. Then, a permutation cannot specify all the initial conditions and realization of the external force $\{p_t\}$ when the length of the permutation tends to infinity.*

Proof. Assume that the underlying dynamics on a one-dimensional interval is not topologically transitive. Then, there is some interval $(a, b) \subset X$ such that any point for the underlying dynamics will not visit the interval (a, b) after any number of iterations, where a and b are some of the time points of the currently given time series up to some length $n > 2$. Therefore, if an initial condition starts within this interval, we cannot refine the uncertainty for such an initial condition even if we prolong the length for the permutation. Since $\{x_t\}$ is not identified, there is no clue for identifying $\{p_t\}$ using the permutation. □

Our theoretical foundation is based on topological transitivity, namely the denseness of orbits: If there is an interval within X, this interval is divided by future points obtained from the underlying dynamics. Thus, this interval is eventually narrowed to a point when the length of the permutations tends to infinity. Once each state is identified, we can also learn the value for dynamical noise because of the property of the embedding between p_t and x_{t+1}.

Moreover, we note that, using the same logic, we can also uniquely specify a point x_k for k $(0 < k < n)$, which is demonstrated in numerical experiments in the next section.

III. NUMERICAL RESULTS

Here, we demonstrate how to use permutations for inferring a state as well as external noise. Our focus is on inferring information regarding the external force. For quantifying the external noise at a particular time, there are two approaches: (i) When we can access a time series of the external noise and (ii) when we cannot access a time series of the external noise.

When we can access a time series $\{p_t\}$ of the external noise p, we can estimate the mean state $M_\pi^p(\kappa)$ for the κ-th relative point of the external noise p by using time segments sharing the same permutation π obtained by time series x in the modelling part of the time series. When we encounter a permutation π in the validating part of the time series, we just need to recall the corresponding mean state $M_\pi^p(\kappa)$.

When we cannot access a time series of the external noise, we try to reproduce the underlying metric space from the generated permutations. We can subdivide this case into two sub-cases. If we assume that the external force is slow, we can directly apply the idea of Ref. [29] to remove the state space information and reproduce the information of the slow external force. If we cannot assume that the external force is slow, then we need to have multiple observation nodes [30, 31] which are subject to the same external force to remove the information of state spaces and reproduce this sudden external force. In either case, we use a recurrence plot [32, 33], which helps us to transform the binary information of whether the two states for the corresponding times are neighbors to a metric space, or a distance matrix.

A. Estimation of states

In addition to the theoretical proofs provided above, we tested our hypothesis numerically. For testing our idea, we used the logistic map [34] and the Hénon map [35] subject to dynamical noise. The logistic map we used is defined as follows:

$$x_{t+1} = (3.7 + \epsilon_t) x_t \left(1 - x_t\right), \tag{6}$$

where ϵ_t is a source of independent uniform noise on $[-0.1, 0.1]$. We chose the initial condition x_0 from a uniform distribution on $[0, 1]$ and observed the time evolution of the variable x_t. Similarly, the Hénon map we used is defined as follows:

$$\begin{aligned} x_{t+1} &= 1 - (1.2 + \eta_t) {x_t}^2 + 0.3 y_t, \\ y_{t+1} &= x_t, \end{aligned} \tag{7}$$

where η_t independently follows a uniform distribution on $[-0.05, 0.05]$. In addition, we choose the initial conditions x_0 and y_0 from the uniform distribution on $[0, 1]$. Therefore, here we are considering dynamical systems subject to dynamical noise and discuss whether we can specify a state x_t by a permutation.

Although our theorem is restricted to one-dimensional interval dynamics, we use the Hénon map to observe whether our claim holds for higher dimensional dynamical systems. We adopt x_t as the observed time series. Our numerical approach aims to represent a time series using a series of permutations (see Fig. 1 for the intuitive illustration). Thus, by specifying a permutation, we can eventually specify both series of states as well as stochastic inputs, simultaneously. Since a permutation eventually specifies a state in the limit for the length of permutation approaching infinity, representing points sharing the same permutation with a point becomes a reasonable approximation. We generated two time series x and x' of the length N from the same system. Here we set $N = 1\ 000\ 000$. For each time series x and x', we also obtained a series of permutations $\{\pi_t(n)\}$ and $\{{\pi'}_t(n)\}$ by using permutations of length n. Then, we use the first time series x and its series of permutations $\{\pi_t(n)\}$ to compute the mean state

$$M^x_\pi(\kappa) = \frac{1}{|\#\{\pi_t = \pi | t = 1, 2, \ldots, N\}|} \sum_{t:\pi_t=\pi} x_{t+\kappa} \tag{8}$$

for the κ-th point of each appearing permutation π. This step is similar to a step of the k-means algorithm [36]. Especially, we define the middle point $K = \lfloor n/2 \rfloor$ of the permutation. These mean states become our estimates for states corresponding to a permutation π since each permutation corresponds to a single initial condition as well as a single series of the external noise in the limit of the size of the permutation approaching to infinity. These means enable us to represent the second time series x' by replacing each permutation ${\pi'}_t(n)$ with the corresponding mean $M^x_{{\pi'}_t(n)}(\kappa)$ state of the κ-th point of permutation ${\pi'}_t(n)$ obtained from the first time series x. (If $\kappa \geq n$, then such an estimation becomes a time series forecast.) Lastly, we evaluate the estimation error

$$\varepsilon^x(\kappa - n{+}1) = E_t\left[\left|{x'}_{t+\kappa} - M^x_{{\pi'}_t(n)}(\kappa)\right|\right] \tag{9}$$

by comparing the second time series x' and its representation $\{M_{{\pi'}_t(n)}(\kappa) | t = 1, 2, \ldots, N - n + 1\}$ constructed by permutations. This approach is called the mean representation [6].

We first estimated states using the mean representation method (Fig. 2). We found that states corresponding to the time period of permutations were estimated more accurately than the cases where we just used the mean states for all over the points of the entire time series.

Moreover, we found a general tendency in the estimation error convergence to 0 with increasing length of permutations (Figs. 3 (a) and (b), for the logistic map [34] and the Hénon

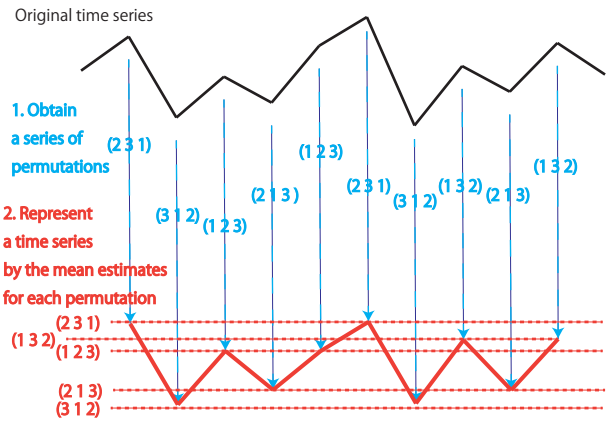

FIG. 1. Schematic for explaining the first numerical approach, the mean representation.

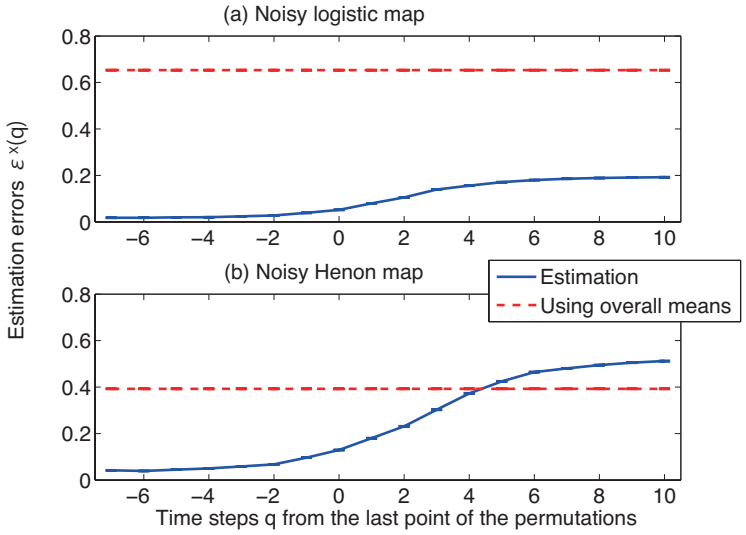

FIG. 2. Estimation errors for the current and future states. Panels (a) and (b) correspond to the cases for the logistic map and Hénon map subject to dynamical noise, respectively. For control, we showed the estimation errors by the overall means that do not depend on the position of the corresponding attractor. Each error bar is obtained from the mean and the standard deviation for ten simulations. Estimations for the future states can be rephrased as "forecasts" of the second time series given the first time series.

map [35], respectively). When we rigorously compared the model of exponential decrease converging to a constant in the limit of $n \to \infty$ with the model of exponential decrease converging to zero using the Akaike information criterion [37], the model of exponential decrease converging to zero was selected for both cases (see Fig. 4). Thus, these results

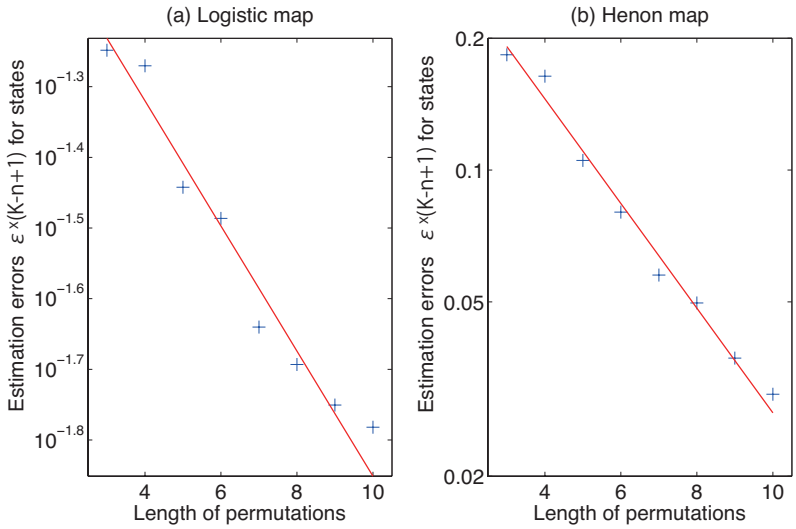

FIG. 3. Estimation error convergence by permutations in (a) the logistic map and (b) the Hénon map. For panels (a) and (b), we used 10 time series of length 1 000 000 to obtain the means for the estimation errors shown by +. The solid lines were obtained by fitting the model of exponential decrease.

imply that a permutation corresponds to an initial condition, or a state, for these models.

Furthermore, the mean representation method was extended so that we considered the means for q steps ahead by defining $\kappa = n - 1 + q$ in Eqs. (8) and (9) to make them "forecasts". Then, we found that we could forecast short-term prediction horizons up to 10 and 4 steps ahead better, in the noisy logistic map (Fig. 2(a)) and the noisy Hénon map (Fig. 2(b)), respectively, than the method of control where we considered the simple means over all the points of the attractor. The accuracy of these forecasts was achieved because the permutations could specify the past states and noise realization, even though uncertainty was generated due to the current and future parts of dynamical noise as well as the sensitive dependence on the initial conditions.

B. Estimation of realization of external force

Theorem 1 implies that we can estimate the realization of the external force when there is a mathematical model for the dynamical system. However, our results imply that even if such a model f is not available, we can estimate the realization of external force in the following two cases:

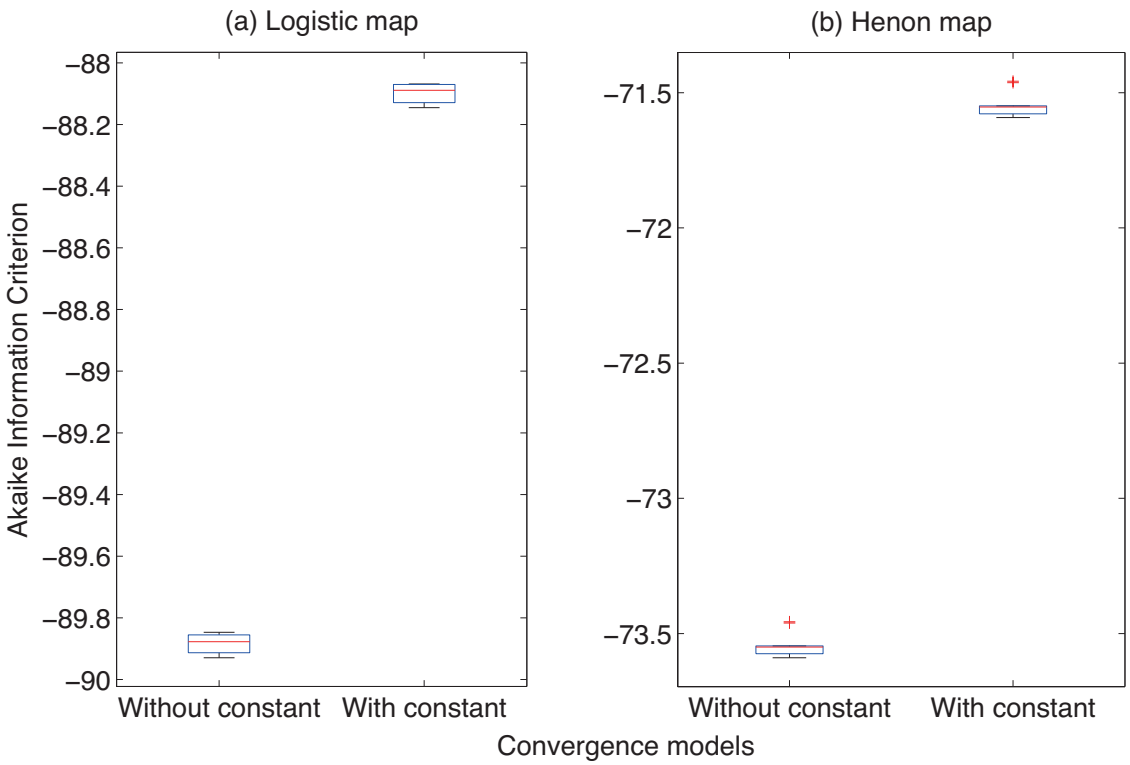

FIG. 4. Comparison of Akaike information criterion between the exponential convergence model without a constant term and with a constant term. Panels (a) and (b) correspond to the logistic map and the Hénon map, respectively. For the exponential convergence model without a constant term, we fitted the error model of $b\exp(-al)$, where l is the length of time series and $b > 0$. For the exponential convergence model with a constant term, we fitted the error model of $b\exp(-al) + c$, where $b, c > 0$.

1. Dynamics of the external force is gradual compared with the driven intrinsic dynamics;

2. We observe multiple time series whose intrinsic dynamics is governed by identical dynamics and are subject to a common external force.

Therefore, Theorem 1 provides a way of obtaining the distribution of external noise as well.

To evaluate this possibility, we have estimated the dynamical noise by using the mean representation method and recurrence plot [32, 33] (See Appendix A). We found that the mean representation method achieved lower estimation errors than merely using the same means over all the permutations when the time steps are those corresponding to the positions of permutations (Fig. 5). In addition, the estimation errors for the noise realization also tend

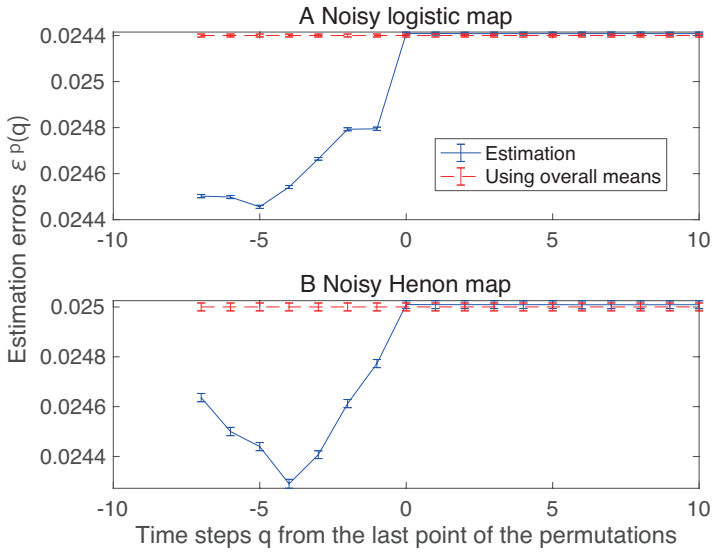

FIG. 5. Estimation errors for the current and future dynamical noise. See the caption of Fig. 2 to interpret the results.

to decrease as the length of permutations increases (Fig. 6). Although we assumed here that a time series of noise realization for modeling is available, this result implies that we could narrow down the possible realization of dynamical noise using permutations. This direction enables us to construct a random dynamical system model.

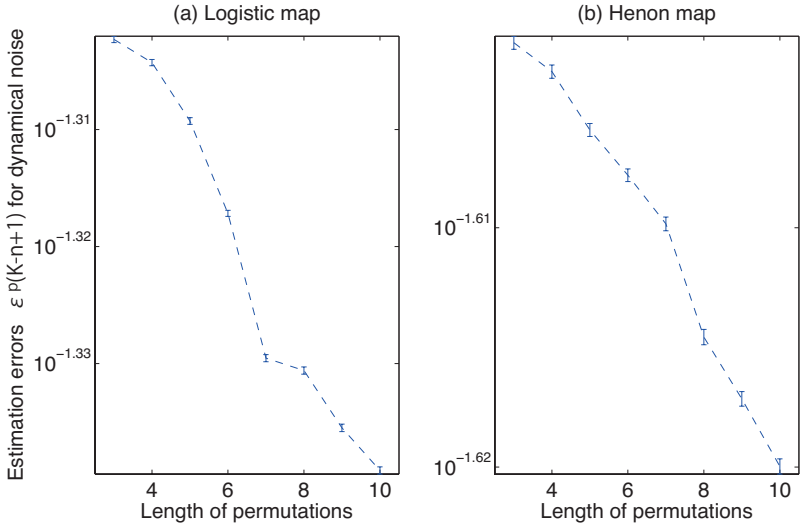

FIG. 6. Estimation error for noise realization in (a) the logistic map and (b) the Hénon map. The error bars show the means and standard deviations for the estimation errors obtained from 10 realizations of time series for each model. The rest of the conditions is the same as Fig. 3.

When we used recurrence plots, we tested with three systems: the logistic maps with the common dynamical noise η_t: For an additive noise case, we use

$$x_{i,t+1} = 3.7x_{i,t}(1 - x_{i,t}) + \eta_t, \tag{10}$$

for $\eta_t \in [0, 0.05]$; for a multiplicative noise case, we use

$$x_{i,t+1} = (3.7 + \eta_t)x_{i,t}(1 - x_{i,t}), \tag{11}$$

for $\eta_t \in [-0.2, 0.2]$.

In the Hénon maps, we use

$$y_{i,t+1} = 1 - 1.2y_{i,t}^2 + 0.3z_{i,t} + \zeta_t, \tag{12}$$

$$z_{i,t+1} = y_{i,t}, \tag{13}$$

for the common additive dynamical noise $\zeta_t \in [-0.1, 0.1]$, or

$$y_{i,t+1} = 1 - (1.2 + \zeta_t)y_{i,t}^2 + 0.3z_{i,t}, \tag{14}$$

$$z_{i,t+1} = y_{i,t}, \tag{15}$$

for the common multiplicative dynamical noise $\zeta_t \in [-0.1, 0.1]$.

Here, we also use a chaotic neuron model [38] to examine a more complicated situation. A chaotic neuron model is an extension of the Nagumo and Sato's neuron model [39] by replacing the Heaviside function with the sigmoid function, which defines whether or not a neuron fires. In a chaotic neuron model [38], we use

$$w_{i,t+1} = 0.5w_{i,t} - \frac{1}{1 + e^{-w_{i,t}/0.04}} + 0.24 + 0.02\sigma_t, \tag{16}$$

for the common additive dynamical noise $\sigma_t \in [-0.02, 0.02]$, or

$$w_{i,t+1} = 0.5w_{i,t} - \frac{1}{1 + e^{-w_{i,t}/(0.04+0.01\sigma_t)}} + 0.24, \tag{17}$$

for the common multiplicative dynamical noise $\sigma_t \in [-0.01, 0.01]$. Namely, states $w_{i,t}$ for multiple neurons at time t are forced by the common dynamical noise σ_t. Here, we assume that each of η_t, ζ_t and σ_t follows the independent and identical uniform noise, respectively. The number L of the maps were decided as the minimum number in the form of 10×2^n with whose corresponding network, each time point is connected with all the other time points within 10 steps. We assigned each of the initial conditions $x_{i,0}, y_{i,0}, z_{i,0}, w_{i,0}$ by the

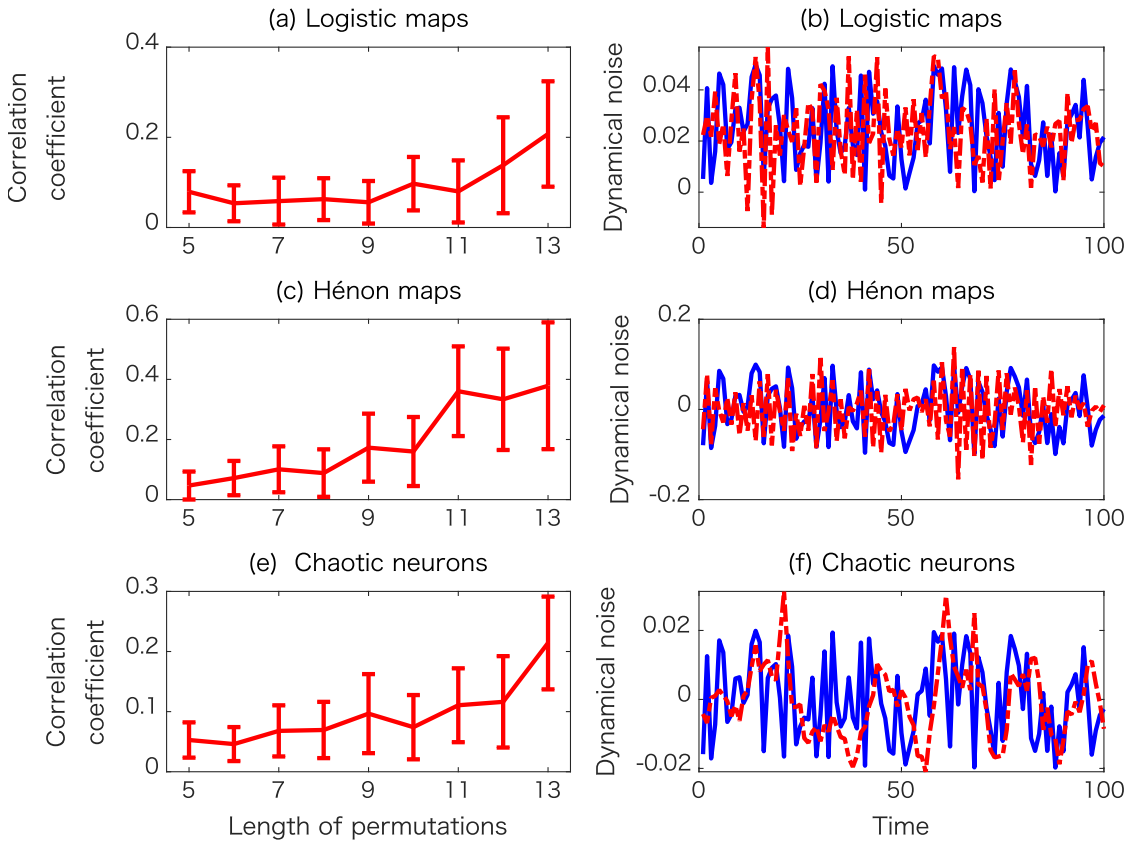

FIG. 7. Estimating the common additive dynamical noise. Panels (a), (c), and (e) show the means and standard deviations for the correlation coefficients between the estimated dynamical noise and its truth calculated over 30 time series, while panels (b), (d), and (f) are examples of estimated dynamical noise estimated for permutations of length 13. In each of the panels (b), (d), and (f), the blue solid line corresponds to the true dynamical noise, while the red dashed line corresponds to one of the reconstructed dynamical noise. Panels (a) and (b) show the examples for the logistic maps, Panels (c) and (d) show the examples for the Hénon maps, and Panels (e) and (f) show the examples for the chaotic neurons. In each simulation, we adjusted the minimum number L of maps as 10×2^n that each time point is connected with all the other time points within 10 steps when we regard the final recurrence plot as a network [31]. Note that there is a degree of freedom for the scaling the estimated dynamical noise. Thus, in Panels (b) ,(d), and (f), we adjusted the reconstructed dynamical noise so that the mean and standard deviation were the same as the actual truth as well as the direction for the reconstructed dynamical noise matches the truth.

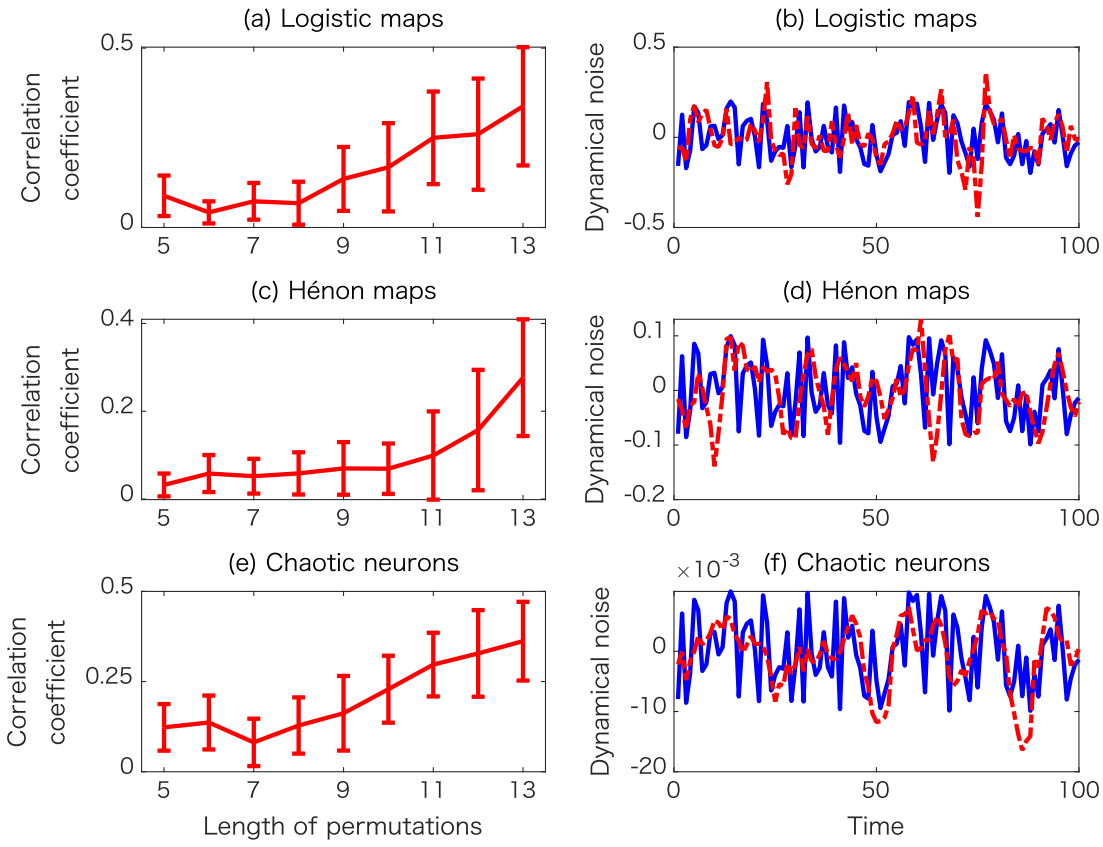

FIG. 8. Same as Fig. 7 but for multiplicative dynamical noise.

uniform distribution between 0 and 1, and generated a time series of length 500 each. We repeated this simulation 30 times to examine the robustness of our findings. We identified the tendency for longer permutations to perform more effectively in estimating the underlying dynamical noise (see panels (a), (c), and (e) of Figs. 7-8) for the additive dynamical noise and multiplicative dynamical noise, respectively. Examples shown in panels (b), (d), and (f) demonstrate that the dynamical noise reconstructed via recurrence plots agreed well with the true dynamical noise.

Overall, these numerical simulations confirmed that a permutation can specify a realization of the external forces, especially dynamical noise, which can be fast in its time scale.

IV. DISCUSSIONS

The goal of this study was to show theoretically and numerically that permutations can uniquely characterize the dynamics and the external forcings in non-autonomous dynamical systems. There are several related studies, and modeling of nonlinear stochastic systems is not new, for example, [40]. Güttler et al. [41] reconstructed the parameter space from the measured time series observed for fixed or slowly varying parameters. Recently, Hamilton et al. [42] proposed a filtering technique with dynamical noise without explicitly modeling the underlying system. The closest study is the one by Seifert et al. [43], where a Langevin equation is assumed for inferring external forces from a measured time series. However, because this work assumes a Langevin equation, the underlying dynamics should be a flow and thus, this technique cannot be applied to a time-discontinuous system. In this sense, the current results could work in a more general setting and provide a rigorous approach for analyzing a non-autonomous system, while its target system could be a map.

Since the number of possible states in permutations increases in a combinatorial manner rather than in an exponential manner, a typical example of which is symbolic dynamics obtained by a generating partition, permutations can overcome dynamical noise by their redundancy [44]. This super-exponential growth is important in enabling a permutation to retain the information regarding both the state space as well as a stochastic input series. If we consider this kind of redundancy, recurrence plots [31–33, 45, 46] can also provide one-to-one correspondence between a time series generated from a stochastic system and its representations.

The current work can be regarded as related to the fundamentals of the mechanism by which permutations can distinguish deterministic systems from stochastic systems [19–25, 47], and validate the analysis of transition matrices [23, 48] induced by a permutation for a stochastic system.

In summary, a permutation can uniquely identify a state for the underlying dynamics even if the dynamics is subject to realization of external force. We provided the mathematical proof (Theorem 1) that the unique specification of a joint set of an initial condition and a realization of the external force by a permutation is equivalent to the condition for the topological transitivity of the given dynamics. We also presented numerical demonstrations using the mean representation as well as the recurrence plots to show that estimating the

realization of the unknown external force is possible. By specifying a permutation, we can ultimately uniquely identify series of states as well as stochastic inputs. Thus, a permutation can be used for time series forecasts of random dynamical systems. From another viewpoint, topological transitivity is a good criterion for evaluating the chaotic nature for the underlying dynamics even when it is generated by random and non-autonomous dynamical systems. Although this point will be further examined in our upcoming research, permutations are certainly expected to provide a rigorous platform for analyzing random as well as deterministic dynamical systems.

SUPPLEMENTARY MATERIAL

The supplementary material includes codes for reproducing numerical calculations and plots presented in Figs. 2-8. Once you unzip the supplementary material, such codes for each figure can be found separated into each folder.

DATA AVAILABILITY STATEMENT

The data that support the findings of this study are available within the article and its supplementary material.

ACKNOWLEDGEMENTS

We would like to thank Editage (www.editage.com) for English language editing. YH is supported by JSPS Grant-in-Aid for Scientific Research (C) JP18K11461. YS is supported by JSPS Grant-in-Aid for Scientific Research (C) No. 18K03441. DF and YS have are supported by a PICS-CNRS grant "Dessert".

Appendix A: Estimation of realization of external force

We estimate dynamical noise from observations from multiple maps by extending the method of Ref. [31] (see Fig. 9). First, we obtained an order recurrence plot [49] using permutations of the same length l (Each permutation $\pi_{i,t}(l)$ corresponds to the information for the joint set $(x_{i,t},\ p_t, p_{t+1}, \ldots, p_{t+l-2})$). An order recurrence plot is a two-dimensional

figure and can be defined as follow:

$$R_i(j,k) = \begin{cases} 1, \text{ if } \pi_{i,j}(l) = \pi_{i,k}(l), \\ 0, \text{ otherwise.} \end{cases} \tag{A1}$$

Then, we applied the OR operations for the order recurrence plots to obtain the resulting recurrence plot [31], which corresponds to the information of $p_t, p_{t+1}, \ldots, p_{t+l-2}$. Namely, we define

$$R(j,k) = \begin{cases} 1, \text{ if } R_i(j,k) = 1 \text{ for some } i = 1, 2, \ldots, I, \\ 0, \text{ otherwise.} \end{cases} \tag{A2}$$

Furthermore, we took the AND operations for $R(j+m, k+m)$ components for each (j,k) for $m = 0, 1, \ldots, l-2$ by duplicating the resulting recurrence plots and applying time delays to obtain the final components $\tilde{R}(j,k)$ for the final recurrence plot. In mathematical language, we define

$$\tilde{R}(j,k) = \begin{cases} 1, \text{ if } R(j+m, k+m) = 1 \text{ for all } m = 0, 1, 2, \ldots, l-2, \\ 0, \text{ otherwise.} \end{cases} \tag{A3}$$

With these AND operations, we could narrow down the information for p_t represented in the final recurrence plot. Lastly, we converted the final recurrence plot to a time series by the method of Ref. [31], which has mathematical support [45, 46]. On this process, first we regard a recurrence plot as a graph. In this graph, a time point corresponds to a node, and points plotted (j,k) and (k,j) correspond to an edge between j and k. Then, we assign to each edge the following local distance d:

$$d(j,k) = 1 - \frac{\sum_l \tilde{R}(j,l)\tilde{R}(k,l)}{\sum_l \tilde{R}(j,l) + \sum_l \tilde{R}(k,l) - \sum_l \tilde{R}(j,l)\tilde{R}(k,l)}. \tag{A4}$$

Second, we obtain the shortest distance between every pair of nodes on this graph, constructing a distance matrix of global distances. For this procedure, we may use Dijkstra's algorithm or Johnson's algorithm [50]. Third, we use multidimensional scaling for converting the distance matrix to a time series. If we extract the most significant component, this component corresponds to the common dynamical noise. Thus, we can transform the information of the recurrence matrix, or the adjacency matrix, to that of the corresponding metric space, resulting in the estimated time series for the common dynamical noise.

---

[1] P. Grassberger and H. Kantz, Phys. Lett. A **113A**, 235 (1985).

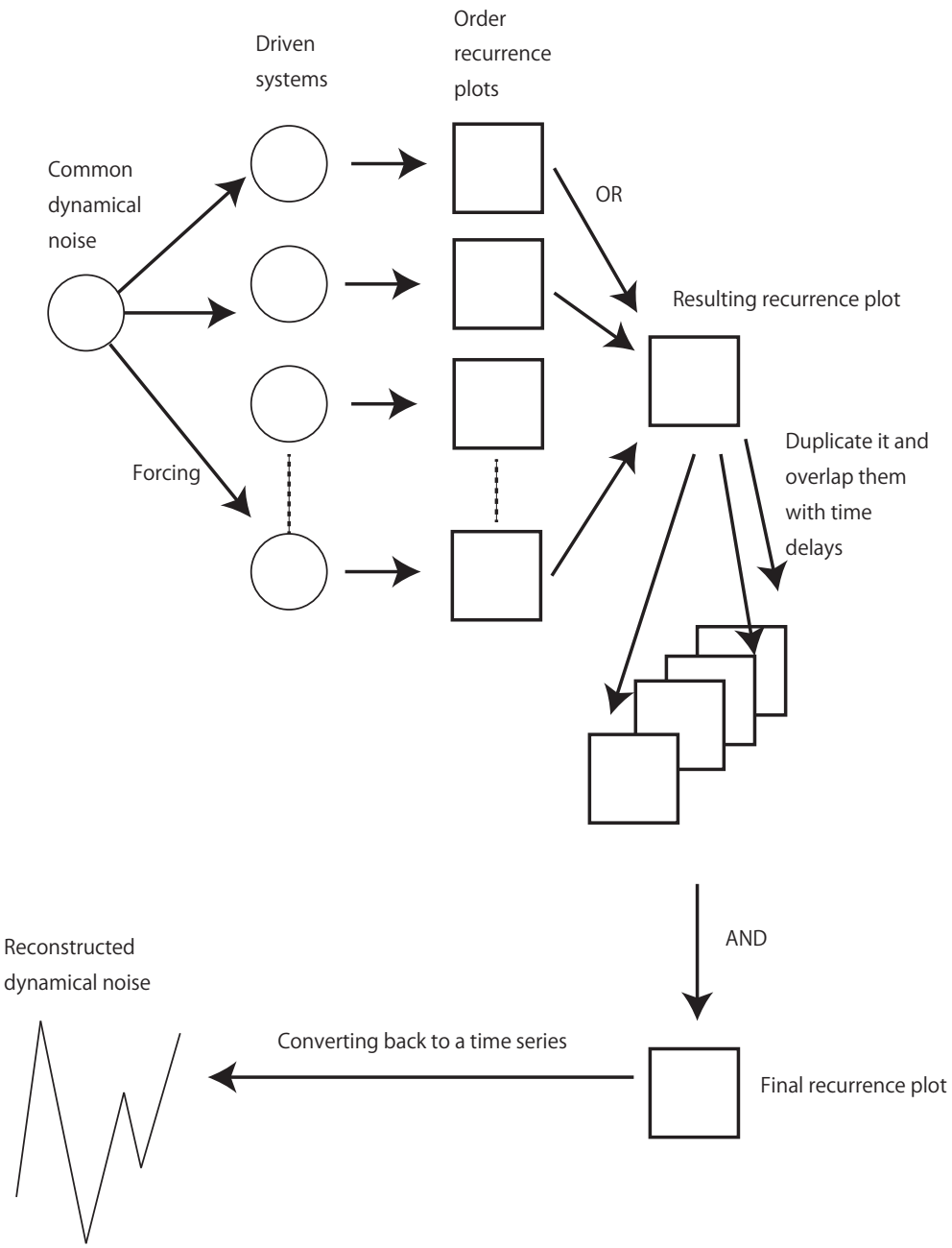

FIG. 9. Schematic for estimating the common dynamical noise using the observations of the driven systems.

[2] R. L. Davidchack, Y.-C. Lai, E. M. Bollt, and M. Dhamala, Phys. Rev. E **61**, 1353 (2000).

[3] J. Plumecoq and M. Lefranc, Physica D **144**, 231 (2000).

[4] J. Blumecoq and M. Lefranc, Physica D **144**, 259 (2000).

[5] M. B. Kennel and M. Buhl, Phys. Rev. Lett. **91**, 084102 (2003).

[6] Y. Hirata, K. Judd, and D. Kilminster, Phys. Rev. E **70**, 016215 (2004).

[7] P. Walters, *An Introduction to Ergodic Theory*, Springer-Verlag, New York, 1982.

[8] H. Chen, S. Kandasamy, S. Orszag, R. Shock, S. Succi, and V. Yakhot, Science 301, 633-636 (2003).

[9] G. Srinivas, D. E. Discher, and M. L. Klein, Nature Materials 3, 638-644 (2004).

[10] M. B. Kennel and A. I. Mees, Phys. Rev. E **61**, 2563 (2000).

[11] M. B. Kennel and A. I. Mees, Phys. Rev. E **66**, 056209 (2002).

[12] Y. Hirata and A. I. Mees, Phys. Rev. E **67**, 026205 (2003).

[13] J. P. Crutchfield and N. H. Packard, Physica **7D**, 201-223 (1983).

[14] R. Shaw, *The Dripping Faucet as a Model Chaotic System*, Aerial Press, (1984).

[15] M. Chekroun, E. Simonnet, and M. Ghil, Physica D **241**, 1685–1700, (2011).

[16] D. Faranda, Y. Sato, B. Saint-Michel, C. Wiertel, V. Padilla, B. Dubrulle, and F. Daviaud, Phys. Rev. Lett. **119**, 014502 (2017).

[17] C. Bandt and B. Pompe, Phys. Rev. Lett. **88**, 174102 (2002).

[18] J. M. Amigó, M. B. Kennel, and L. Kocarev, Physica D **210**, 77-95 (2005).

[19] J. M. Amigó, S. Zambrano, and M. A. F. Sanjuán, EPL **83**, 60005 (2008).

[20] C. W. Kulp, J. M. Chobot, B. J. Niskala, and C. J. Needhammer, Chaos **26**, 023107 (2016).

[21] M. McCullough, K. Sakellariou, T. Stemler, and M. Small, Chaos **26**, 123103 (2016).

[22] K. Sakellariou, M. McCullough, T. Stemler, and M. Small, Chaos **26**, 123104 (2016).

[23] A. A. B. Pessa and H. V. Ribeiro, Phys. Rev. E **100**, 042304 (2019).

[24] Y. Hirata and M. Shiro, Phys. Rev. E **100**, 022203 (2019).

[25] Y. Hirata, M. Shiro, and J. M. Amigó, Entropy **72**, 713 (2019).

[26] J. M. Amigó and M. B. Kennel, Physica D **231**, 137-142 (2007).

[27] M. R. Muldoon, D. S. Broomhead, J. P. Huke, and R. Hegger, Dynamics and Stability of Systems **13**, 175-186 (1998).

[28] G. Froyland, Extracting Dynamical Behavior via Markov models, in Ed. A. I Mees, *Nonlinear Dynamics and Statistics*, Birkhäuser, Boston, 2000, pp. 281-321.

[29] Y. Hirata and K. Aihara, Phys. Rev. E **96**, 032219 (2017).

[30] T. Sauer, Phys. Rev. Lett. **93**, 198701 (2004).

[31] Y. Hirata, S. Horai, and K. Aihara, Eur. Phys. J. Spec. Top. **164**, 13-22 (2008).

[32] J.-P. Eckmann, S. O. Kamphorst, and D. Ruelle, Europhys. Lett. **4**, 973 (1987).

[33] N. Marwan, M. C. Romano, M. Thiel, and J. Kurths, Phys. Rep. **438**, 237-329 (2007).

[34] R. May, Nature **261**, 459 (1976).

[35] M. Hénon, Commun. Math. Phys. **50**, 69 (1976).

[36] N. Gershenfeld, The Nature of Mathematical Modeling, Cambridge University Press, Cambridge, UK, 1998.

[37] H. Akaike, IEEE Trans. Automatic Control **19**, 716 (1974).

[38] K. Aihara, T. Takabe, and M. Toyoda, Phys. Lett. A **144**, 333-340 (1990).

[39] J. Nagumo and S. Sato, Kybernetik **10**, 155-164 (1972).

[40] S. Allie, A. Mees, K. Judd, and D. Watson, Phys. Rev. E **55**, 87-93 (1997).

[41] S. Güttler, H. Kantz, and E. Olbrich, Phys. Rev. E **63**, 056215 (2001).

[42] F. Hamilton, T. Berry, and T. Sauer, Eur. Phys. J. Spec. Top. **226**, 3239-3250 (2017).

[43] M. Siefert, A. Kittel, R. Friedrich, and J. Peinke, Europhys. Lett. **61**, 466-472 (2003).

[44] T. Kohda, Y. Horio, Y. Takahashi, and K. Aihara, Int. J. Bifurcat. Chaos **22**, 1230031 (2012).

[45] Y. Hirata, M. Komuro, S. Horai, and K. Aihara, Int. J. Bifurcat. Chaos **25**, 1550168 (2015).

[46] A. Khor and M. Small, Chaos **26**, 043101 (2016).

[47] S. Still and J. P. Crutchfield, Santa Fe Institute Working Paper 07-08-020, 2018.

[48] M. McCullough, K. Sakellariou, T. Stemler, and M. Small, Chaos 27, 035814 (2017).

[49] A. Gorth, *Phys. Rev. E* **72**, 046220 (2005).

[50] T. H. Cormen, C. E. Leiserson, R. L. Rivest and C. Sten, Introduction to Algorithms, Third Edition, The MIT Press, 2009.